Studies of turbulence and its modelling through large eddy- and direct numerical simulation

by Krister Alvelius

October 1999
Technical Reports from
Royal Institute of Technology
Department of Mechanics
SE-100 44 Stockholm, Sweden

Typsatt i \mathcal{AMS} - $\mathbb{A}T_{E}X$.

Akademisk avhandling som med tillstånd av Kungliga Tekniska Högskolan i Stockholm framlägges till offentlig granskning för avläggande av teknologie doktorsexamen fredagen den 1:a oktober 1999 kl 10.15 i Kollegiesalen, Administrationsbyggnaden, Kungliga Tekniska Högskolan, Valhallavägen 79, Stockholm.

©Krister Alvelius 1999 Norstedts Tryckeri AB, Stockholm 1999

Studies of turbulence and its modelling through large eddy- and direct numerical simulation

Krister Alvelius

Department of Mechanics, Royal Institute of Technology SE-100 44 Stockholm, Sweden

Abstract

This thesis deals with numerical simulations of turbulence in simple flow cases. Both homogeneous turbulence and turbulent plane channel flow are computed, either through direct numerical simulations (DNS) or through large eddy simulations (LES) where the effect of the smallest scales, the subgrid-scales (SGS), are modelled. The simple flow cases allow the use of pseudo spectral methods which yield a very accurate discretization and allow the focus to be put on the turbulence dynamics rather than the details of the numerical methods. The DNS methodology is a cornerstone in turbulence research and allows for detailed studies of turbulence dynamics and structures. DNS has been performed for the rotating channel flow, where many complicated features of turbulence have been explored. New insights into the generation of large elongated structures in this flow were gained through these computations. DNS was also used for statistical stationary homogeneous turbulence, where a forcing method was developed which extends the range of useful DNS. The DNS results from the rotating channel flow have also been used in the development of SGS models for LES. In the homogeneous turbulence case LES is used with simple SGS models to investigate the features of high Reynolds number turbulence dynamics, and to determine weather accurate high Reynolds number calibrations of standard statistical turbulence models can be obtained. The stochastic approach is adopted to describe the random behaviour of the subgrid-scales in the plane channel flow. This strongly increases the variance and reduces the length scale of the model, while the mean behaviour is unchanged. A large effort has been put in the optimization of the numerical codes on various super computers to increase the effective Reynolds number in the simulations.

Descriptors: Turbulence, Direct numerical simulation, Large eddy simulation, Homogeneous flow, Plane channel flow, subgrid-scales, parallel computers

Preface

This thesis considers Large eddy simulation and direct numerical simulation of simple flows. The thesis is based on the following papers.

Paper 1. Alvelius, K. and Johansson, A. V. and Hallbäck, M. 1999 'An LES study of the Smagorinsky model and calibration of slow-pressure strain rate models'

submitted to European Journal of Mechanics/B Fluids

Paper 2. Alvelius, K. 1999 'Random Forcing of three-dimensional homogeneous turbulence'

in Physics of Fluids A, 11 (7), 1880–1889

Paper 3. Alvelius, K. and Johansson, A. V. 1999 'LES computations and comparison with Kolmogorov theory for two-point pressure-velocity correlations and structure functions for globally anisotropic turbulence' accepted for publication in Journal of Fluid Mechanics

- Paper 4. Alvelius, K. 1999 'A pseudo spectral method for LES of homogeneous turbulence'
- **Paper 5.** Alvelius, K. and Johansson, A. V. 1999 'Stochastic Modelling in LES of a turbulent channel flow with and without system rotation'
- **Paper 6.** Alvelius, K. and Johansson, A. V. 1999 'DNS of rotating turbulent channel flow at various Reynolds numbers and Rotation numbers' submitted to Journal of Fluid Mechanics
- **Paper 7.** Alvelius, K. and Skote, M. 1999 'The performance of a spectral simulation code for turbulence on parallel computers with distributed memory' submitted to SIAM Journal on Statistical and Scientific Computing

The papers are here re-set in the present thesis format. Some of them are based on publications in conference proceedings [3], [2], [4], [7].

Contents

Preface		iv		
Chapter	1. Introduction	1		
Chapter	2. Filtering the turbulence field	5		
2.1.	Governing equations	5		
2.2.	Subgrid-scale stress models	10		
2.3.	Stochastic differential equations	17		
Chapter	3. Numerical implementation	20		
3.1.	Numerical discretization	20		
3.2.	Computer optimization	21		
Chapter	4. Probing homogeneous turbulence with LES	23		
4.1.	LES of decaying homogeneous turbulence	23		
4.2.	Calibration of RANS models using LES	24		
4.3.	Numerical experiments of turbulence inertial range dynamics	26		
Chapter	5. LES and DNS of turbulent channel flow	29		
5.1.	Turbulent plane channel flow	29		
5.2.	Stochastic SGS modelling	31		
Chapter	: 6. Concluding remarks	32		
${ m Acknowledgments}$				
Bibliography				

- Paper 1: An LES study of the Smagorinsky model and calibration of slow-pressure strain rate models
- Paper 2: Random Forcing of three-dimensional homogeneous turbulence
- Paper 3: LES computations and comparison with Kolmogorov theory for two-point pressure-velocity correlations and structure functions for globally anisotropic turbulence

v

- Paper 4: A pseudo spectral method for LES of homogeneous turbulence
- Paper 5: Stochastic Modelling in LES of a turbulent channel flow with and without system rotation
- Paper 6: DNS of rotating turbulent channel flow at various Reynolds numbers and rotation numbers
- Paper 7: The performance of a spectral simulation code for turbulence on parallel computers with distributed memory

Introduction

Turbulence is characterized by fluctuating motions with a large range of scales. Most flow states in nature are turbulent, e.g. the atmospheric flow and the wind blowing air close to the earth surface. In the flow around a moving object, turbulence is usually triggered. With the development of modern transportation vehicles, such as cars and aeroplanes, the need to find optimal body shapes with good aerodynamic properties, e.g. low air resistance, arose. Since those flows usually are turbulent, tools for predicting turbulence are needed. Already in the classical experiments of the flow in a long tube by Reynolds [56] in the 1880:s the irregular motion of turbulence was observed. This kind of chaotic behaviour yields a vigorous mixing of the fluid which is very important in many engineering applications such as the turbulent mixing of air and gasoline in a combustion engine. Indeed, the turbulent diffusion is usually much larger than the molecular one.

For Newtonian fluids the flow motion is described by the Navier-Stokes equations together with suitable boundary conditions. In three-dimensional flows the non-linear term in the Navier-Stokes equations transfers energy from the large, energy producing scales, to the small dissipative scales. The largest scale in the flow is typically determined by the characteristic size of the flow domain, and the smallest dissipative scales are determined by the kinematic viscosity and the dissipation rate (the rate of energy transfer into heat, which in 'equilibrium' equal the transfer from large to small scales). The large and small scales can formally be defined as the integral length scale Λ and the Kolmogorov micro length scale $\eta = (\nu/\epsilon^3)^{1/4}$ (see e.g. Tennekes and Lumley [64]). The Reynolds number

$$Re = \left(\frac{\Lambda}{\eta}\right)^{4/3},\tag{1}$$

is hence a measure of the range scales in the flow. The large and small length scales are also associated with the corresponding large and small time scales respectively.

The Navier-Stokes equations need to be discretized, both in time and space, in order to yield a solution. The discretization gives algebraic equations with many degrees of freedom that need to be solved at each discrete time in a direct numerical simulation (DNS). The range of spatial scales, in all three spatial directions, needs to be resolved by the collocation of the discretization points

1

which from (1) is related to the Reynolds number as $N \sim Re^{9/4}$. Even for moderate Reynolds number this yields a very large number of degrees of freedom, challenging for even the fastest super-computers available today. The time step in the numerical integration is determined by the stability condition of the numerical method, the CFL condition $\Delta t \leq \min(\Delta x_i/u_i)$ (see e.g. Fletcher [20]), where Δx_i is the grid size, u_i the velocity component and the minimum is taken over the whole computational domain and in all spatial directions. This yields a time step which usually is significantly smaller than the smallest dissipative scale. The time integration has to be performed over time scales larger than the largest time scale in the flow $T \sim \Lambda/U$, where U is a characteristic large velocity scale, in order to significantly reduce (or preferably eliminate) the influence of the non-physical initial conditions. Hence, the number of iterations needed for a DNS scales as $T/\Delta t \sim Re^{3/4}$ (where it has been assumed that $\Delta x_i \sim \eta$ and that the largest values $u_i \sim U$). Altogether, the large number of degrees of freedom and the large number of discrete integration steps gives that not many problems of engineering interest can be solved by direct integration of the discrete Navier-Stokes equations.

To this day the statistical approach, where the ensemble averaged field is considered, is the most dominating. The mean velocity field is governed by the Reynolds averaged Navier-Stokes (RANS) equations. In the RANS equations a large part of the information about the flow is averaged out, and put into the Reynolds stress tensor, which is unknown and needs to be modeled in terms of averaged quantities. The solution is often stationary and relatively smooth allowing for much fewer collocation points resulting in a significant reduction of the computational effort. In addition, statistical quantities are constant in homogeneous directions and in which cases fewer dimensions can be considered. However, the model for the Reynolds stress tensor adds an uncertainty to whether the solution appropriately describes the flow. The models have to be calibrated in many different flow configurations, and sometimes model parameters are tuned for the specific problem type considered.

In another approach, which has become wide spread with the development of modern computers, only the smallest scales are modeled in so called large eddy simulations (LES). This is formally done by filtering the flow field with a low pass filter in order to damp out the small scale fluctuations. The LES field is then smoother than the corresponding DNS field with the filter width as the characteristic length scale to be resolved by the collocation points. This reduces the computational effort, allowing for higher Reynolds number simulations. The filtered velocity field is governed by the filtered Navier-Stokes equations, and the effect from the so called subgrid-scales enters through the subgrid scale (SGS) stress tensor. Since a major part of the flow is resolved by the filtered field the importance of the SGS stress tensor is much smaller than the Reynolds stress tensor in the RANS approach. Also, since the subgrid scales are much

smaller than the energy producing large scales they are expected to be relatively universal, allowing for simpler models to be used. The information of the flow configuration enters directly through the dynamic response of the filtered field. Although the models may be simpler in the sense that they are expected to have the same behaviour in different flow cases, they should also capture the fluctuating behaviour of the real SGS stresses, with e.g. the correct variance, length and time scales. They should mimic the somewhat chaotic behaviour inherent in the smallest scales of turbulence. This suggests that the area of stochastic processes, and stochastic differential equations is a useful tool in the development of good SGS models.

LES is under development to become an engineering tool for complex flows. The early efforts in LES (in the early 1970:s) where focused on the atmospheric boundary layer applications although the simple case of channel flow was used as a test case, see e.g. Deardorff [17] and the early model work by Smagorinsky [61]. Examples of cases where LES has been successful are the simple channel flow [50], the backwards facing step [9], the flow past a cube attached to a channel wall [37] and developing jets [53]. The channel flow work of Moin and Kim [50] became a landmark in LES and also triggered much of the following DNS work in e.g. turbulent channel flow (see Kim et al. [30]). LES can also be used as a tool for the study of turbulence dynamics [12], [6] and be used for calibration of RANS models [5]. Although LES is believed to yield good predictions of the flow behaviour, there is always, as in the Reynolds averaged case, an uncertainty of the SGS model which only can be eliminated in DNS. The various models are usually tested with the aid of DNS data from simple flow cases. Hence, the DNS tool is still very important, and is to be considered as a cornerstone in the area of turbulence research.

In research both DNS and LES are usually performed in simple flow domains in order to simplify the numerical implementation, and also reduce the associated numerical errors that always follow from the numerical discretization. Simple domains allow for higher Reynolds numbers in the simulations as compared to more complex flows. They also allows isolation of certain specific effects that are of interest, simplifying the procedure of interpreting the results and drawing correct conclusions. Two of the most simple flow cases are isotropic or anisotropic homogeneous flow and the plane channel flow. They can be discretized through spectral methods which are very accurate, and most of the results in the literature are from these test cases.

In the early LES of plane channel flow by Deardorff [17] the number of grid points was 6720. Moin and Kim [50] used 5×10^5 grid points in their LES, and later Kim *et al.* [30] used 4×10^6 grid points to perform well resolved DNS. More recent DNS [51] at higher Reynolds numbers were performed with up to 38×10^6 grid points. In the present thesis LES of homogeneous turbulence have been performed with up to 17×10^6 spectral modes (see paper 3), and DNS

of plane channel flow have been performed with up to 24×10^6 spectral modes (see paper 6). The 3/2-dealiasing method which is used gives the corresponding physical space representation on 58×10^6 and 53×10^6 grid points for the two cases respectively.

Filtering the turbulence field

2.1. Governing equations

The flow state is, in the incompressible case, described completely by the velocity, \mathbf{u} , and pressure, p, fields, which time development are governed by the Navier-Stokes equations and the continuity equation

$$\frac{\partial u_i}{\partial t} + u_j \frac{\partial u_i}{\partial x_j} = -\frac{1}{\rho} \frac{\partial p}{\partial x_i} + \nu \frac{\partial^2 u_i}{\partial x_j \partial x_j}, \tag{2}$$

$$\frac{\partial u_j}{\partial x_j} = 0, (3)$$

where ρ is the fluid density and ν is the kinematic viscosity. LES solves for a filtered velocity field. A filter may be either temporal or spatial. The latter is the most commonly considered, and the spatial filtering of a quantity f is denoted by an overbar – and is defined in physical space as

$$\bar{f}(\mathbf{x}) = \int_{-\infty}^{\infty} f(\mathbf{x}') G(\mathbf{x}, \mathbf{x}') d^3 x', \tag{4}$$

where G is a filter function that satisfies the condition

$$\int_{-\infty}^{\infty} G(\mathbf{x}, \mathbf{x}') d^3 x' = 1.$$
 (5)

The filter should reduce the small scale fluctuations, giving a smoother field that can be represented on a coarser numerical grid than the unfiltered field. The filter operator is characterized by a filter width Δ , which is representative of the smallest length scale that can be retained in the filtered field. Since the filtered field should be resolved by the numerical mesh the filter width is often associated with the grid scale. The scales that are not included in the filtered field are therefore referred to as subgrid scales (SGS). The SGS part is defined as

$$f' = f - \bar{f},\tag{6}$$

so that the sum of the resolved (filtered) field and the SGS field equals the original unfiltered field. For a general filter function we have

$$\overline{f'} = \overline{f} - \overline{\overline{f}} \neq 0. \tag{7}$$

Hence, the filter operator also alters scales that are within the filter width. If the filter function can be written as $G(\mathbf{x} - \mathbf{x}')$ it is said to be homogeneous. For

Filter	Filter function $G(\mathbf{x} - \mathbf{x}')$	Fourier transform $\hat{G}(\mathbf{k})$
Spectral cut-off	$\Pi_{i=1}^{3} \frac{\sin(k_{c}(x_{i}-x'_{i}))}{\pi(x_{i}-x'_{i})}$	$\begin{cases} 1 & \text{if } k_i \le k_c \\ 0 & \text{otherwise} \end{cases}$
Gaussian	$\left(\frac{6}{\pi\Delta^2}\right)^{3/2} \exp\left(\frac{-6 \mathbf{x}-\mathbf{x}' }{\Delta^2}\right)$	$\exp\left(\frac{-\Delta^2 k^2}{24}\right)$
Top-hat	$\begin{cases} 1/\Delta^3 & \text{if } x_i - x_i' \le \frac{1}{2}\Delta \\ 0 & \text{otherwise} \end{cases}$	$\Pi_{i=1}^{3} \frac{\sin\left(\frac{1}{2}\Delta k_{i}\right)}{\frac{1}{2}\Delta k_{i}}$

Table 1 The filter function.

homogeneous filters the filter operator and the spatial derivative commute. The filtering can also (for homogeneous filters) be performed in Fourier space where each Fourier component of \bar{f} is

$$\widehat{\bar{f}}(\mathbf{k}) = \widehat{G}(\mathbf{k})\widehat{f}(\mathbf{k}),\tag{8}$$

where the hat \hat{d} denotes the Fourier transform and \mathbf{k} is the wavenumber vector. The condition (5) translates in spectral space to $\hat{G}(0) = 1$, and a reduction of the small scale fluctuation is obtained if $\hat{G}(\mathbf{k}) < 1$ for large wavenumbers \mathbf{k} .

The most commonly considered filters are the spectral cut-off filter, the Gaussian filter and the top-hat filter (table 1). The spectral cut-off filter in table 1 is referred to as 'cubic'. It is also common to consider 'spherical' spectral cut-off filters with the Fourier transformed filter function

$$\hat{G}(\mathbf{k}) = \begin{cases} 1 & \text{if } |k| \le k_c \\ 0 & \text{otherwise} \end{cases}$$
 (9)

Filtering the Navier-Stokes equations and the continuity equation using a homogeneous filter one obtains the LES equations for the filtered velocity and pressure fields

$$\frac{\partial \bar{u}_i}{\partial t} + \bar{u}_j \frac{\partial \bar{u}_i}{\partial x_j} = -\frac{1}{\rho} \frac{\partial \bar{p}}{\partial x_i} + \nu \frac{\partial^2 \bar{u}_i}{\partial x_j \partial x_j} - \frac{\partial \tau_{ij}}{\partial x_j}, \tag{10}$$

$$\frac{\partial \bar{u}_k}{\partial x_k} = 0, \tag{11}$$

where $\tau_{ij} = \overline{u_i u_j} - \overline{u_i \overline{u}_j}$ is the SGS stress tensor which contains the information about the effect of the small subgrid scales on the filtered field. The LES equations are similar to the NS equations, and may be solved with similar numerical methods together with a model for τ_{ij} . The SGS stress tensor can be modeled at different levels of complexity, just as the Reynolds stresses in the Reynolds averaged approach. However, the filtered field contains more information about the flow than the corresponding averaged field which can be used in the modeling. One example is the Germano identity (see (17) below), which has no counterpart in the Reynolds averaged approach. The Germano identity gives an algebraic relation between the SGS stresses at different filter levels, which is used to determine model constants in the SGS stress models.

In order to solve the equations for the filtered field boundary conditions for \bar{u}_i and \bar{p} are needed. Since the field at the wall is averaged over some domain close to the wall it is not obvious what the boundary conditions for \bar{u}_i and \bar{p} should be.

The SGS stress tensor can be modeled either directly, in terms of the filtered field, or through a transport equation where, due to the closure problem of turbulence, new unknown terms will appear that needs to be modelled. A common approach to develop RANS models at different levels is to study the transport equation for the unknown quantity. This may also be used in SGS modelling. It is common to consider the following decomposition of the SGS stress tensor

$$\tau_{ij} = \overline{u}_i \overline{u}_j - \overline{u}_i \overline{u}_j + \overline{u}_i u'_j + \overline{u}_j u'_i + \overline{u'_j u'_i}, \tag{12}$$

where the first two terms are referred to as the Leonard stresses, the second two are the cross stresses and the last is the Reynolds stresses. It should be noted that the Leonard stresses and cross stresses are not Galilean invariant under system translatation, only the sum of them are [63], [28]. In this expression the difference between τ_{ij} and $\overline{u'_i u'_j}$ clearly reflects the property of the filtering in (7). Although the different parts in (12) can be modelled separately they are usually treated and modelled together. In order to obtain a general approach, transport equations are formed for the generalized central moments defined by

$$\tau(u_i, u_j) \equiv \overline{u_i u_j} - \bar{u}_i \bar{u}_j, \tag{13}$$

$$\tau(u_i, u_j, u_k) \equiv \overline{u_i u_j u_k} - \bar{u}_i \tau(u_j, u_k) - \bar{u}_j \tau(u_k, u_i) - \bar{u}_k \tau(u_i, u_j) - \bar{u}_i \bar{u}_j \bar{u}_k,$$
(14)

$$\tau(u_i, u_j, u_k, u_l) \equiv \dots \tag{15}$$

For homogeneous filters Germano [21] derived

$$\tau(u_{i}, u_{j})_{,t} + \bar{u}_{k} \tau(u_{i}, u_{j})_{,k}
= -(\tau(u_{i}, u_{j}, u_{k}) + \tau(p, u_{i})\delta_{jk} + \tau(p, u_{j})\delta_{ik} - \nu\tau(u_{i}, u_{j})_{,k})_{,k}
+ 2\tau(p, s_{ij}) - 2\nu\tau(u_{i,k}, u_{j,k})
- \tau(u_{i}, u_{k})\bar{u}_{j,k} - \tau(u_{j}, u_{k})\bar{u}_{i,k},$$
(16)

where the notation $\partial/\partial t=_{,t}$ and $\partial/\partial x_k=_{,k}$ has been introduced. The left hand side is the material derivative. The first term on the right hand side is a transport term, the second is a pressure-strain rate term, the third is a viscous destruction term and the fourth is a production term. Transport equations for the unknown central moments in this equation may be derived in an analogous way. If the filter has the property $\overline{f'}=0$, we get $\tau(u_i,u_j)=\overline{u'_iu'_j}$ and $\tau(u_i,u_j,u_k)=\overline{u'_iu'_ju'_k}$ and equation (16) reduces to the transport equation for the Reynolds stresses in the RANS approach. This is true for e.g. the spectral cut-off filters and the standard ensemble average, where the main difference between those two cases is that the spectral cut-off filters yields rapidly fluctuating solutions compared to the slowly varying statistical solution.

There is an algebraic relation between the SGS stresses at different filter levels. Denote a new filter operator by a tilde $\tilde{}$, and define the sub-test scale (STS) stress tensor at the $\tilde{}$ filter level as $T_{ij} = \widetilde{u_i u_j} - \tilde{u}_i \tilde{u}_j$. The following relation, the Germano identity [22], is readily obtained

$$T_{ij} - \tilde{\tau}_{ij} = \widetilde{u_i u_j} - \tilde{u}_i \tilde{u}_j - \widetilde{u}_i \tilde{u}_j - \widetilde{u}_i u_j + \widetilde{u}_i u_j = \widetilde{u}_i u_j - \tilde{u}_i \tilde{u}_j \equiv L_{ij}.$$
 (17)

 L_{ij} can be calculated exactly in LES since \bar{u}_i is known and the $\tilde{}$ filter may be applied explicitly. The relation can be used to determine SGS model parameters by substituting the model expressions into (17). Usually a similarity assumption, where the model parameter value is the same on both filter levels, is made.

- 2.1.1. Complex flows. The typical use of LES is in complex flows, where the geometrical effects enters directly through the resolved field. These cases requires the use of non-homogeneous filters which introduces extra unknowns [25], which have to be put into an extra term in (10). Close to solid walls the large energy carrying scales become relatively small, which implies that the filter scale needs to be reduced compared to that for the outer flow. This generates strained and strongly distorted grids (filters). At high Reynolds number flows the extra grid refinement that is needed in LES close to the walls gives a significant increase in computational effort, and special near wall treatment may be required.
- **2.1.2.** The filtering problem. The solution of the LES equations gives the filtered fields, $\bar{\mathbf{u}}$ and \bar{p} , and for appropriate interpretation of the results the filter function G should be known. Some statistics of the velocity field u_i can be obtained exactly by defiltering \bar{u}_i if G is known, e.g. the kinetic energy spectrum can be computed through

$$E(k) = |\hat{G}(k)|^{-2} E^f(k), \tag{18}$$

where E^f is the energy spectrum computed of the filtered field. It is, however, impossible to recover the complete unfiltered velocity field, since there are infinitely many different fields \mathbf{u} which give the same filtered quantity $\bar{\mathbf{u}}$.

Ideally, the information which is lost in the filter should be recovered in the model of τ_{ij} . In practice, however, it is difficult to determine the correspondence between the filter and SGS stresses. The only way to know how the filter affects the SGS stress tensor seems to be to explicitly filter an unfiltered velocity field, either from an experiment or from a DNS.

Although all the information about the filtering is put into the SGS stress tensor, commonly used SGS models do not damp the velocity fluctuations sufficiently at the filter level, which implies the need of an extra explicit filtering not connected to the model. The explicit filtering could be applied at each time step in the LES by integrating the filter kernel over the whole velocity field. This is referred to as explicit filtering in the literature [44]. It can also be performed by the numerical method, where e.g. a second order central difference scheme corresponds to a top hat filter. This is referred to as implicit filtering [52]. The

numerical grid in the finite difference scheme will not allow scales in the flow smaller than the grid-size and will therefore act as a filter. For spectral cut-off filters the relation $\overline{\overline{f}} = \overline{f}$ holds and the truncation of the Fourier series at each time step guarantees a spectral cut-off filter.

The explicit filtering suggests that one may have some control over the choice of filter. However, since the LES velocity field does not equal the unfiltered field it is difficult to interpret what you get after the explicit filtering has been applied.

2.1.3. The nature of the SGS stresses. The SGS stresses act on the smallest resolved scales in the flow. When these are locally much smaller than the largest scales, their behaviour can be expected to be relatively universal allowing simple SGS stress models to be used. The SGS stresses do, however, fluctuate in time and space with certain characteristic time and length scales. Besides the mean behaviour, these fluctuating characteristics are expected to have an important effect on the flow.

The non-linear terms, in the three dimensional Navier-Stokes equations, transfer, on average, energy from the large scale motions to the small scales. This average transfer, which is the most important feature to capture in LES with an SGS model, is the outcome of two large, but partially cancelling effects: a forward energy transfer and a somewhat smaller backward transfer. A physical backscatter from unresolved to resolved scales would correspond to a locally negative dissipation by the SGS stress tensor.

The local value of τ_{ij} at a spatial point is the result of two large terms which are averaged with some weight function (the filter function) around that point. The behaviour of τ_{ij} will thus depend on the filter function. The SGS stress tensor is positive semidefinite if and only if the filter function, $G(\mathbf{x}, \mathbf{x}')$, is nonnegative for all values of \mathbf{x} and \mathbf{x}' [65]. For a positive semidefinite tensor τ_{ij} the following relations are valid

$$\tau_{ii} \ge 0, \quad |\tau_{ij}| \le (\tau_{ii}\tau_{jj})^{1/2}, \quad \det(\tau_{ij}) \ge 0 \quad i, j \in \{1, 2, 3\}$$
(19)

(no summation over repeated indices 'i' and 'j' here). The relations in (19) can be used to give constraints for the SGS model when non-negative filters are used. The Gaussian and the top-hat filters are non-negative for all values of \mathbf{x} and \mathbf{x}' while the spectral cut-off filters are not.

2.1.4. The physical and numerical resolution. A large part of the inertial sub-range needs to be resolved for the LES to be relatively independent of the SGS stress model. In flows with complicated geometries, e.g. around a car or an aeroplane, it is not possible to ensure sufficient resolution everywhere in the flow due to limitations in computer power. In these cases a relatively large part of the velocity field is put into the sub-grid scale and it is important to have a good model which captures the main physical features of the flow.

The errors in an LES come both from the physical resolution determined by the filter width, through the SGS stress model, and from the numerical resolution of the smallest LES scale. It is desirable to have a numerical method of such accuracy that the numerical errors are much smaller than the SGS stress term. If one uses a lower order method the filter width should be larger than the numerical grid [44]. However, for a given problem to be solved with a specific computer, LES can be considered as a method of resolving the field as well as possible and trying to compensate for the errors coming from the unresolved field through the SGS stresses. In order to make the numerical errors small the filter scale should be resolved. For a given computer and a given size of the numerical grid the only way of resolving the filter scale better is to make it larger, since the smallest grid size is fixed. This will, however, make the errors from the SGS model larger.

In LES research it is important to be able to separate different effects from each other and the numerical errors have to be controlled. In an industrial application however, the best possible prediction of a certain quantity is required. This implies that there is a matter of balancing the numerical grid size compared to the filter width to minimize the total error.

2.2. Subgrid-scale stress models

In LES the resolved velocity field contains more information as compared to the mean velocity field in the RANS approach. This information can be used in the SGS models. Zero equation models, e.g. the Smagorinsky model [61], the spectral model [13], the mixed model [8], the stress similarity model [43] and the velocity estimation model [18] are the most commonly used so far in LES. In homogeneous turbulence the main task of the SGS model is to dissipate energy from the filtered field in a proper way, and simple models that predict a correct energy transfer to the sub-grid scales are normally sufficient. Close to solid walls special treatment, e.g. with damping of model parameters, is usually needed.

The common eddy viscosity models are absolutely dissipative and do not yield backscatter. Other standard models have been found to yield backscatter in the sense of locally negative dissipation. I has been argued that standard deterministic models cannot capture the random fluctuating behaviour of the SGS stresses, and do not give physically correct backscatter [10], [58]. Instead a stochastic term which models the random behaviour of backscatter should be added to the model for the SGS stress tensor. Stochastic processes have successfully been used by several authors [11], [46], [58] to improve the SGS stress model. In particular, the backscatter seems to be an important factor close to solid walls [46], [55] and models that take it into account have been found to work well [46].

2.2.1. The Smagorinsky model. The Smagorinsky model [61] is based on an eddy viscosity formulation, and reads

$$\tau_{ij} = \frac{1}{3} \tau_{kk} \delta_{ij} - 2\nu_T \bar{s}_{ij}, \qquad (20)$$

where $\bar{s}_{ij} = (\bar{u}_{i,j} + \bar{u}_{j,i})/2$ is the filtered strain rate tensor. The eddy viscosity can from dimensional arguments be estimated by $\nu_T \sim u(k_c)/k_c$, where $u(k_c)$ stands for a velocity scale at the filter level, indicated by the wavenumber k_c . The velocity scale is estimated through the kinetic energy spectrum, E, as

$$u(k_c) \sim \sqrt{E(k_c)k_c},\tag{21}$$

and if k_c lies in an inertial sub-range we get

$$\nu_T \sim \epsilon^{1/3} k_c^{-4/3}$$
. (22)

The dissipation by the subgrid scales in the LES is given by $\epsilon = 2\nu_T \bar{s}_{pq} \bar{s}_{pq}$ and $k_c \sim \Delta^{-1}$, where Δ is the filter width. This gives an expression for the eddy viscosity based on a local estimation of the dissipation

$$\nu_T = (C_s \Delta)^2 (2\bar{s}_{pq} \bar{s}_{pq})^{1/2}, \tag{23}$$

where C_s is the Smagorinsky constant. The trace τ_{kk} in the model is treated together with the pressure according to $\bar{q} \equiv \bar{p}/\rho + \tau_{kk}/3$ and remains an unknown quantity.

The value of the Smagorinsky constant has been a frequent issue of investigation. Lilly [38] derived a high Reynolds number expression

$$C_s = \frac{1}{\pi} \left(\frac{2}{3\alpha}\right)^{3/4},\tag{24}$$

where α is the Kolmogorov constant. It has, however been found that if the value of α obtained from an LES with the Smagorinsky model is inserted in the Lilly formula then the computed value of C_s becomes inconsistent with the one used in the simulation. In paper 1 a more thorough analysis were performed to get the expression

$$C_s = \frac{1}{f\pi} \left(\frac{2}{3\alpha}\right)^{3/4},\tag{25}$$

where f is a correction function which depends on the low wave number energy spectrum shape, the ratio between third and second order moments and the actual shape of the filter function. Through this expression the previous inconsistencies of the Lilly formula were resolved.

The value of the filter width Δ in the Smagorinsky model is for isotropic grids naturally chosen proportional to the grid spacing. For anisotropic meshes Deardorff [17] suggested the choice $\Delta_{eq} = (\Delta_x \Delta_y \Delta_z)^{1/3}$, which is reasonable for moderately strained meshes. Scotti *et al.* [59] derived, from integration of energy spectra over the spectral filter domain, corrections to Δ_{eq} for strongly strained meshes. In the dynamic approach C_s and Δ are essentially treated together, and determined locally in the flow by the filtered field.

2.2.2. The spectral model. The spectral model is formulated in spectral space, and is closely related to the Fourier transformed filtered Navier-Stokes equations

$$\frac{d\hat{\bar{u}}_i}{dt} + i \, k_k \, \widehat{\bar{u}_i \bar{u}_j} = -\frac{i}{\rho} k_i \hat{\bar{p}} - \nu \, k^2 \hat{\bar{u}}_i - i \, k_k \hat{\tau}_{ik}. \tag{26}$$

The spectral model [13] reads

$$i k_k \hat{\tau}_{ik} = \nu_T(k) k^2 \hat{\bar{u}}_i, \tag{27}$$

$$\nu_T(k) = \text{Ko}^{-3/2} \left[0.441 + 15.2 \exp\left(\frac{-3.03k_c}{k}\right) \right] \sqrt{\frac{E(k_c, t)}{k_c}},$$
 (28)

and it is derived for a 'spherical' spectral cut-off filter with a cut-off wavenumber k_c and should therefore be used only together with a spectral method, where the spectral cut-off gives a truncation of the Fourier series for the velocity and the pressure fields. In this formulation the divergence of the complete SGS stress tensor is modeled, not only the deviatoric part. The contribution from SGS stresses to the pressure in the Poisson equation enters as $k_i k_j \hat{\tau}_{ij}$. This term is zero for the spectral model and it does not influence the pressure directly, which, however, the true SGS stress tensor does.

In the derivation of (28) it has been assumed that k_c lies in a region with a $k^{-5/3}$ slope of the energy spectrum. For the more general case where k_c lies in a region with a k^{-m} slope, where m < 3, Métais and Lesieur [49] derived

$$\nu_T = 0.31 \frac{5 - m}{m + 1} \text{Ko}^{-3/2} \left[1 + 34.5 \exp\left(\frac{-3.03k_c}{k}\right) \right] \sqrt{\frac{E(k_c, t)}{k_c}}.$$
 (29)

This expression becomes equivalent to (28) when m = 5/3.

2.2.3. The structure function model. The spectral model has been extended to a physical space implementation in the structure function model [49], where again the divergence of the SGS stresses is modelled as

$$\frac{\partial}{\partial x_j} \tau_{ij} = 2 \frac{\partial}{\partial x_j} \left[\nu_t^{SF} \bar{s}_{ij} \right] + \nu_t^{(2)} \frac{\partial^2}{\partial x_j^2} \bar{u}_i, \tag{30}$$

where ν_T^{SF} and $\nu_T^{(n)}$ are expressed in terms of e.g. the local structure function \bar{F}_2 averaged for separations smaller than the filter width

$$\bar{F}_2(\mathbf{x}, \Delta x, t) = \langle ||\bar{\mathbf{u}}(\mathbf{x}, t) - \bar{\mathbf{u}}(\mathbf{x} + \mathbf{r}, t)||^2 \rangle_{r = \Delta x}.$$
 (31)

Compte $et\ al.$ [15] introduced the selective and filtered structure function model in order to reduce the sensitivity to large scale fluctuations in the original approach.

2.2.4. The mixed model and the stress similarity model. It has been observed in experiments and DNS calculations that there seems to be a rather high correlation between the SGS stresses, τ_{ij} , and

$$\overline{\overline{u}_i \overline{u}_j} - \overline{\overline{u}}_i \overline{\overline{u}}_j. \tag{32}$$

It could therefore be a good idea to model the SGS stresses in terms of this expression. However, despite the high correlation with τ_{ij} the expression (32) is not dissipative enough, and a combination of (32) and the Smagorinsky model is often used in the mixed model of Bardina *et al.* [8]

$$\tau_{ij} = -2\nu_T \bar{s}_{ij} + C_b (\overline{u}_i \overline{u}_j - \overline{u}_i \overline{u}_j). \tag{33}$$

This model depends directly on the type of filter used, and for the spectral cutoff filters the term $\overline{u}_i\overline{u}_j - \overline{u}_i\overline{u}_j$ is identically zero. Another model, the stress similarity model, based on the same type of ideas, has been proposed by Liu *et al.* [43]

$$\tau_{ij} = -2\nu_t \bar{s}_{ij} + C_l (\widetilde{\bar{u}_i \bar{u}_j} - \tilde{\bar{u}}_i \tilde{\bar{u}}_j). \tag{34}$$

In this form both models (33) and (34) give explicit expressions for the trace of the SGS stress tensor and they also allow backscatter, i.e. energy transfer from the sub-grid scales to the resolved scales. Recently the performance of different scale similarity models was investigated in different flows by Sarghini *et al.* [57].

2.2.5. The velocity estimation model. In the velocity estimation model by Domaradzki [18] the definition of τ_{ij} is used together with a model v_i for the complete velocity field

$$\tau_{ij} = \overline{v_i v_j} - \overline{v}_i \overline{v}_j. \tag{35}$$

It was concluded that the main energy transfer between the resolved and subgrid scales is performed by scales that are only twice as small as the filter width [18]. The estimated field \mathbf{v} is hence represented on a mesh that is twice as fine as for the filtered field $\bar{\mathbf{u}}$, and is determined by requiring that

$$\bar{v}_i = \bar{u}_i, \quad \tilde{v}_i = \tilde{\bar{u}}_i \tag{36}$$

at each spatial point of the filtered field, where the filter $\tilde{}$ is wider than the original. The coefficients for the wavenumbers k greater than k_c are corrected by giving them the same phase as the computed non-linear term $\overline{u_iu_j}$, while the amplitude is kept unchanged. This yields a model that has a high correlation with the true stresses, as was the case also for the mixed model, and also provides sufficient net dissipation.

A similar approach in which the definition of τ_{ij} is used with a modelled complete velocity field was proposed by Geurts [23] in the so called inverse modeling. He emphasized that the filter should appear explicitly in the model, and for a given filter the complete velocity field can be realized accurately from the

filtered velocity field down to scales of the filter width. An approximate inversion method for a top-hat filter was considered, and the resulting model showed a better performance than the mixed model by Bardina [8].

2.2.6. The dynamic Smagorinsky model. In the dynamical approach the Germano identity (17) is used to determine the Smagorinsky model constant locally in time and space. If a scale similarity assumption is made the model for the STS stress tensor T_{ij} may be written as

$$T_{ij} = \frac{1}{3} T_{kk} \delta_{ij} - 2\nu_T \tilde{\tilde{s}}_{ij}, \tag{37}$$

$$\nu_T = (C_s \tilde{\Delta})^2 (2\tilde{s}_{pq} \tilde{s}_{pq})^{1/2},$$
(38)

where $\tilde{\Delta}$ is the filter width corresponding to the \tilde{a} filter. The ratio between the two filter widths $\tilde{\Delta}/\Delta$ is usually set to two. Now we put $C_s^2 \equiv C$ which is allowed to be negative. Insert the models for τ_{ij} and T_{ij} into equation (17) to obtain [22]

$$L_{ij} - \frac{1}{3}\delta_{ij}L_{kk} = 2CM_{ij},\tag{39}$$

$$M_{ij} = (\tilde{\Delta})^2 \beta_{ij} - (\Delta)^2 \tilde{\alpha}_{ij}, \tag{40}$$

where

$$\beta_{ij} = (2\tilde{\bar{s}}_{pq}\tilde{\bar{s}}_{pq})^{1/2}\tilde{\bar{s}}_{ij}, \quad \alpha_{ij} = (2\bar{s}_{pq}\bar{s}_{pq})^{1/2}\bar{s}_{ij}. \tag{41}$$

Here it has been assumed that C is varying slowly enough in space so that it is possible to exclude it from the filtering. This is an over-determined system with five equations and one unknown, C. The least square method suggested by Lilly [39] may be applied to yield a solution

$$C = \frac{1}{2} \frac{L_{lm} M_{lm}}{M_{pq} M_{pq}},\tag{42}$$

which fluctuates in time and space, and may be both positive and negative. A negative value of C gives a negative dissipation which causes numerical problems, and therefore both the numerator and denominator in the expression (42) are usually averaged in homogeneous directions to increase the numerical stability. In lack of homogeneous directions temporal averaging may be applied [48]. Another approach to achieve numerical stability is to restrict the value of C to a certain interval [52]. If the constant is not assumed to be slowly varying it has to be kept inside the filtering [24]. This results in an equation which involves calculation of a Fredholm integral of the second kind

$$C(x) = \int \kappa(x, y)C(y)dy + f(x)$$
(43)

where

$$f(x) = \frac{1}{\alpha_{kl}(x)\alpha_{kl}(x)} [\alpha_{ij}(x)L_{ij}(x) - \beta_{ij}(x) \int \widetilde{G(y,x)}L_{ij}(y)dy], \quad (44)$$

$$\kappa(x,y) = \frac{1}{\alpha_{kl}(x)\alpha_{kl}(x)} [\widetilde{G(y,x)}\alpha_{ij}(x)\beta_{ij}(y) + \widetilde{G(y,x)}\alpha_{ij}(y)\beta_{ij}(x)$$

$$- \beta_{ij}(x)\beta_{ij}(y) \int \widetilde{G(z,x)}\widetilde{G(z,x)}dz]. \quad (45)$$

The value C can be calculated iteratively [54] by substituting the value of C from the previous time step into the integral to get a new value of C. This process can be repeated with the new value of C until the iteration converges.

The performance of the dynamical model depends on the filter that is used. It has been found that the spectral cut-off filters do not work as well in combination with the dynamical model as the Gaussian and top-hat filters [43]. This is due to the lack of coupling between the resolved field and the SGS field caused by the spectral cut-off.

2.2.7. Transport equation models. Analogous to the Reynolds averaged approach one may derive transport equations either for the SGS stresses directly or for the quantities in the SGS stress models. Yoshizawa [68] used a transport equation for $\overline{u'_k u'_k}$ to define a velocity scale for the eddy viscosity in the Smagorinsky model. To define an eddy viscosity one needs a velocity and a length scale. In LES the characteristic length scale of the largest subgrid scales is given explicitly by the filter width, Δ . There are two natural quantities from which it is possible to form a velocity scale, the generalized SGS kinetic energy $K_{\rm sgs} = \tau_{kk}/2$ and the 'SGS turbulent kinetic energy' $\overline{u'_k u'_k}/2$. The first condition in (19) suggests that K_{sgs} is a suitable quantity to solve for with a transport equation, which is readily obtained by taking the trace of equation (16), only in the case of positive filters. For non-positive filters, e.g. the spectral cut-off filters, $K_{\rm sgs}$ may be negative locally in the flow which makes the modeling of the unknowns in the equation more difficult, and it might be preferable to use a transport equation for $u'_i u'_i$ in that case. The transport equation can be combined with more complicated algebraic relations than the ordinary eddy viscosity hypothesis to give the SGS stress tensor.

A transport equation for τ_{kk} may effectively be used together with a dynamic SGS model [10]. Since the value of τ_{kk} is known from the transport equation there is a limit, when using positive filters, on how much backscatter that can be allowed. A locally negative value of C corresponds to backscatter, which will reduce τ_{kk} , and if the negative value is persistent τ_{kk} will approach zero which will eliminate the backscatter. It is also possible to use the dynamical approach to determine model constants in the transport equation analogous as for the Smagorinsky model [10]. This approach was adopted by Sohankar et al. [62] in the LES of flow around a square cylinder, using the dynamic Smagorinsky model, with the velocity scale in the eddy viscosity determined by K_{sgs} . The

modelled equation for K_{sgs} was solved with a dynamic determination, not only for the Smagorinsky model parameter but also for the included model parameter for the dissipation of K_{sgs} which was determined locally without averaging.

2.2.8. Stochastic models. The main motivation to use stochastic models has been to increase the chaotic behaviour and to obtain physically correct backscatter [58].

Leith [36] proposed to model the backscatter through the divergence (acceleration) of τ_{ij} as the curl of a random vector potential ϕ_i

$$-\frac{\partial \tau_{ij}}{\partial x_i} = \epsilon_{ijk} \frac{\partial \phi_j}{\partial x_k},\tag{46}$$

where, from dimensional arguments

$$\phi_k = C_b |\bar{s}\Delta t|^{3/2} \left(\frac{\Delta}{\Delta t}\right)^2 g_i \tag{47}$$

and g_i are unit Gaussian random numbers, generated independently at each time and grid point. To this model the Standard Smagorinsky model is added, which yields a positive net dissipation, and through this formulation the correct k^4 energy spectrum shape of the backscatter is obtained. The zero time correlation gives the explicit time step Δt dependence in the expression for ϕ_i . This yields a non-zero net contribution to the backscatter from the acceleration-acceleration correlation, which is $C_b^2 |\bar{s}|^3 \Delta^4 \sum \operatorname{Var}[g_i]$, where $\operatorname{Var}[g_i]$ is the variance of g_i .

The same approach, to express the divergence of τ_{ij} as the curl of a vector potential, was used by Mason and Thomson [46], but a finite time correlation was considered. However, in the simulations, the temporal correlation was from simplicity chosen to be zero. The results of their simulation was significantly improved close to the solid wall when the stochastic model was included.

Schumann [58] stressed the importance of a finite model timescale to obtain correct influence on particularly higher order statistics. The random part of the model was formulated as

$$R_{ij} = \gamma \left(v_i v_j - \frac{2}{3} K_{\text{sgs}} \delta_{ij} \right), \tag{48}$$

where γ is a model parameter in the range 0 and 1. The random velocity components v_i are given by

$$v_i = \left(\frac{2K_{\text{sgs}}}{3}\right)^{1/2} X_i,\tag{49}$$

where X_i is a stochastic process with unit variance. Schumann chose the time scale of the stochastic process to

$$\tau_v = c_{\tau v} \Delta / K_{\text{sgs}}^{1/2}, \tag{50}$$

where K_{sgs} is determined through a modelled transport equation and $c_{\tau v}$ is of order unity. When the timescale of the stochastic model is finite it is important that it is considered in the Lagrangian sense.

2.2.9. Evaluation of SGS stress models. When developing SGS stress models there is a continuous need to evaluate the performance. This can either be done in so called a priori tests, where a resolved velocity field is used to compute various SGS quantities through the definition, or in actual LES with the model. In the a priori tests the resolved velocity field is usually obtained from DNS [47], [14], although experimentally measured fields have also been used [43]. The a priori test offers a fast method to statistically evaluate the prediction of different quantities, with the reservation that the modelled quantities are evaluated from a field slightly different from the supposed LES field. In addition, only the statistical predictions of the model is captured, not the dynamic interaction with the filtered field in the solution process. In order to know how the model really performs, actual LES have to be carried out, and compared with either DNS or experiments.

2.3. Stochastic differential equations

Stochastic processes have to be considered when stochastic modelling is used. Many stochastic processes can be generated through stochastic differential equations (SDE) on the form

$$\int_0^t \mathrm{d}X(s) = \int_0^t \mu(s)\mathrm{d}s + \int_0^t \sigma(s)\mathrm{d}W(s),\tag{51}$$

where W is a Wiener process, and μ and σ are two stochastic processes adapted to the sigma algebra generated by $\{W_s\}_{s\leq t}$. For a more detailed description see e.g. Øksendal [34]. The SDE (51) is usually written on a simper form as

$$dX(t) = \mu(t)dt + \sigma(t)dW(t). \tag{52}$$

The Wiener process was originally developed to model the irregular behaviour of Brownian motion. In recent years the theory of stochastic differential equations have gained large interest with the appearance of different derivatives on the financial market, such as the pricing of call options for the stock market with the famous Black-Scholes formula. Stochastic analysis can also be used to prove various features of some partial differential equations through the Feynman-Kac representation. In turbulence research it has been used to derive realizability conditions for second-moment closures in the RANS approach [19].

Due to the irregularity of the Wiener process, the ordinary Riemann integral cannot be used. Instead the Itô integral is defined, from which the Itô calculus follows. The Itô formula gives a rule for differentiating stochastic processes Z(t) = f(t, X(t)) where X(t) is given on the form (52), which due to the large irregularities of W becomes different than the ordinary rules for deterministic functions. The differential of a stochastic process Z can formally be obtained

by standard Taylor expansion up to second order terms together with the basic computational rules

$$(dW)^2 = dt$$
, $(dt)^2 = 0$, $dtdW = 0$. (53)

The statistical properties, given by the expectation value E, of a stochastic process X, which differential can be written on the form (52), can easily be obtained by using the fact that

$$E\left[\int_0^t X(s) dW(s)\right] = 0. (54)$$

The properties of X is determined by μ and σ . When stochastic processes are used in SGS stress modelling, they have to be considered in a Lagrangian sense, with extra transport terms added to the SDE.

2.3.1. Example: random forcing. The flow driven by a random volume force f with the property $\langle f(t)f(s)\rangle = \mathrm{Var}[f]\delta(t-s)$ is closely related to that of Brownian motion. Consider the simple differential equation

$$\frac{\mathrm{d}u(t)}{\mathrm{d}t} = f(t), \quad u(0) = 0,$$
 (55)

which captures the main features of the random forcing methodology. Since f(t) is independent of u(t) the solution is directly given by

$$u(t) = \int_0^t f(s) \mathrm{d}s. \tag{56}$$

The mean power input by the random force is

$$\frac{1}{2}\frac{\mathrm{d}}{\mathrm{d}t}\langle u(t)u(t)\rangle = \int_0^t \langle f(t)f(s)\rangle \mathrm{d}s = \mathrm{Var}[f]\int_0^t \delta(t-s)\mathrm{d}s = \frac{1}{2}\mathrm{Var}[f]. \tag{57}$$

The discrete form of (55) reads

$$u_{n+1} = u_n + f_n \Delta t, \tag{58}$$

and yields the power input

$$\frac{1}{2}\frac{u_{n+1}^2 - u_n^2}{\Delta t} = \frac{1}{2}f_n^2 \Delta t + u_n f_n.$$
 (59)

On average $u_n f_n$ is zero and in order for the discrete equation to approximate the solution of (55) it is necessary that $f_n = (\Delta t)^{-1/2} X$, where X is a stochastic variable with Var[X] = Var[f].

The random Brownian motion can in the simplest case be described by the ${
m SDE}$

$$dv(t) = dW(t), \quad v(0) = 0,$$
 (60)

where v here is the position of a particle. It has the trivial solution

$$v(t) = \int_0^t dW(s) = W(t).$$
 (61)

Define the 'kinetic energy' as $K_v = v^2/2$. The Itô computational rules gives that K_v is described by the SDE

$$dK_v(t) = v(t)dv(t) + \frac{1}{2} (dv(t))^2 = v(t)dW(t) + \frac{1}{2} dt.$$
 (62)

This yields the solution

$$K_v(t) = \int_0^t v(s) dW(s) + \frac{1}{2}t,$$
 (63)

and from the computational rules above it follows that the mean power input is 1/2 since the expectation value of the integral is zero. From (61) v can be written as

$$v(t_{n+1}) = v(t_n) + \int_{t_n}^{t_{n+1}} dW(s) = v(t_n) + \Delta W_n,$$
(64)

where $\Delta W_n = W(t_{n+1}) - W(t_n)$. By comparing the discrete solution to u with the expression for v it follows that they are equal if $f_n \Delta t = \Delta W_n$. The process ΔW_n has zero mean and variance $t_{n+1} - t_n = \Delta t$. Thus if $\operatorname{Var}[f] = 1$ the discrete solution to u 'equals' the solution for v.

The method of random forcing, hence, corresponds to a large scale 'Brownian motion' of the velocity field, which generates turbulence fluctuations at smaller scales through energy cascading action of the nonlinear terms. The 'constant' power input is hence dissipated by the small scales which prevents the energy in the large scales to grow unlimitedly. If the random force is homogeneous in time a statistically stationary state will be reached, where the large scale production is balanced by the small scale dissipation.

Numerical implementation

3.1. Numerical discretization

The LES of a specific problem is closely linked to the numerical implementation. Since the typical mesh spacing is of the same order as the filter width discretization errors may be relatively large. For complex flows it is important to have a numerical method that works well together with the LES, and do not add large undesired numerical errors that may reduce the performance of the LES. In the present work the focus is put on the LES method, and to investigate how well an LES can do under the ideal conditions of negligible numerical errors, and to get a better understanding of the role of the SGS stresses. Therefore, the simple flow cases of homogeneous turbulence and turbulent plane channel flow are used, with geometries that allow for very accurate numerical discretizations.

Fourier series expansion of the flow field can with advantage be used in the spatial directions where periodic boundary conditions are imposed. If a quantity u(x) is L_x -periodic, i.e if $u(x+L_x)=u(x)$ for all x, it can be expanded in a Fourier series

$$u(x) = \sum_{l=-\infty}^{\infty} \hat{u}(l) \exp(ik_l x), \tag{65}$$

where $k_l = l2\pi/L_x$, i = (0,1) and $\hat{u}(l)$ is the Fourier transform of u(x). For reasonably smooth functions u(x) the contribution to the sum usually becomes very small for high values of |l|. In a numerical discretization only a finite number of terms $|l| \leq N$ are included in the summation to yield the approximation $u^N(x) \approx u(x)$, where the contribution of the remaining is negligible. In this formulation the spatial derivative of a function is simply obtained as

$$\frac{\mathrm{d}}{\mathrm{d}x}u^{N}(x) = \sum_{l=-N}^{N} ik_{l}\hat{u}(l) \exp\left(ik_{l}x\right),\tag{66}$$

which is exact for u^N . Hence, this procedure does not introduce any additional errors from the spatial differentiating, as compared to finite difference methods which introduce errors related to the grid size $\Delta x = L_x/2N$. Typically finite difference methods may be of second order, which means that the finite difference errors will be proportional to $(\Delta x)^2$.

In homogeneous turbulence simulations Fourier series representation is used in all three spatial directions since they are all periodic. In the plane channel flow it is not suitable to use Fourier series representation in the non-homogeneous wall-normal direction. Instead Chebyshev series is used [45], which allows more rapid fluctuations of the discretized function close to the walls. The location of the collocation points in physical space gives that Fourier transforms actually can be used to obtain the Chebyshev coefficients.

A velocity-vorticity formulation is used to eliminate the fluctuating pressure from the governing equations, and the original four equations are reduced to two equations for two unknowns. The nonlinear terms from the NS equations are computed in physical space, where the velocity field is represented on a 3/2 finer mesh, resulting in a 3/2-energy conserving dealiasing method. Fast Fourier transforms are used when changing between the spectral space and physical space representations.

The discrete time integration procedures are implicit for the linear parts of the NS equations and explicit for the nonlinear parts. For the homogeneous case this gives that the Fourier coefficients are uncoupled and explicit expressions may be obtained. In the plane channel flow, the spatial derivatives in the wallnormal direction gives due to the use of Chebyshev series coupled coefficients. This results in a tri-diagonal equation systems which have to be solved at each iteration.

3.2. Computer optimization

The progress made in the area of turbulence simulations is related to the development of super computers. Modern super computers usually have several processors on which the program should run in parallel. The large primary memory of the computer is either shared by all processors or distributed locally on each processor. Generally a simulation code cannot run on both types of systems without modifications. A processor has either scalar or vector registers. A scalar processor performs operations on one element at the time with fast access to memory, whereas a vector processor performs operations on several elements at the same time.

The homogeneous simulation code has been parallelized to run on both distributed and shared memory systems (paper 4). The performance on vector processor machines (e.g. Cray J90 and C90) is very good due to the long loops associated with the spectral formulation. On scalar processor machines (e.g. IBM SP2 and Cray T3E) the performance is relatively low due to the intense memory access of the fast Fourier transforms. The scalar processor machines, however, often have a large number of processors which gives an overall high performance.

The plane channel flow simulation code was already optimized for shared memory systems with vector processors. In paper 7 a low storage parallelization

method for distributed memory and scalar processor machines is developed and tested. The scalability with the number of processors used was found to be excellent while the intense memory access in the FFT reduces the single processor performance. However, due to the large number of processors the overall computer speed becomes relatively high, 3.5 Gflop/s (floating point operations per second) on 64 processors on an IBM SP2.

Probing homogeneous turbulence with LES

4.1. LES of decaying homogeneous turbulence

Homogeneous turbulence is an important simple flow case in which turbulence models can be tested and developed. It allows the use of pseudo spectral methods in all spatial directions which yields a very accurate discretization. A globally homogeneous flow can of course never be realized in an experimental set up. However, a flow can often be considered to be locally homogeneous, where the quantities vary slowly relative to typical turbulence length scales, e.g. in the center of a wind-tunnel with zero pressure gradient at sufficient high Reynolds number.

Decaying homogeneous turbulence is perhaps the simplest flow case and has been studied by a large number of authors, both experimentally and numerically [16], [26], [12], [60]. In this case there are no mean velocity gradients and the budget equation for the turbulence kinetic energy K reduces to

$$\frac{\mathrm{d}K}{\mathrm{d}t} = -\epsilon \tag{67}$$

where ϵ is the dissipation rate of K. The turbulence can either be isotropic or anisotropic in which case the pressure-strain rate redistributes the energy between the different velocity components towards an isotropic state.

Although being a very simple case, good simulations of decaying turbulence can be difficult to perform. For small times the flow state will strongly depend on the initial conditions. These are usually not physically correct, which means that the turbulence need some time to develop in the simulation. During this time the typical large length scale grows, the Reynolds number decreases, and in the case of anisotropic turbulence the degree of anisotropy is reduced. Hence, in this case the effective time of a useful simulation is often limited. The time needed to obtain a physically correct turbulent state will to a large extent depend on the initial kinetic energy spectrum shape. In decaying homogeneous turbulence a more or less self-similar decay of the kinetic energy spectrum is observed [12]. This is associated with self-similar decay of K and ϵ , motivated by the form of the budget equation (67), in which case the ratio

$$C_{\epsilon 2} = \frac{K/\frac{\mathrm{d}K}{\mathrm{d}t}}{\epsilon/\frac{\mathrm{d}\epsilon}{\mathrm{d}t}} \tag{68}$$

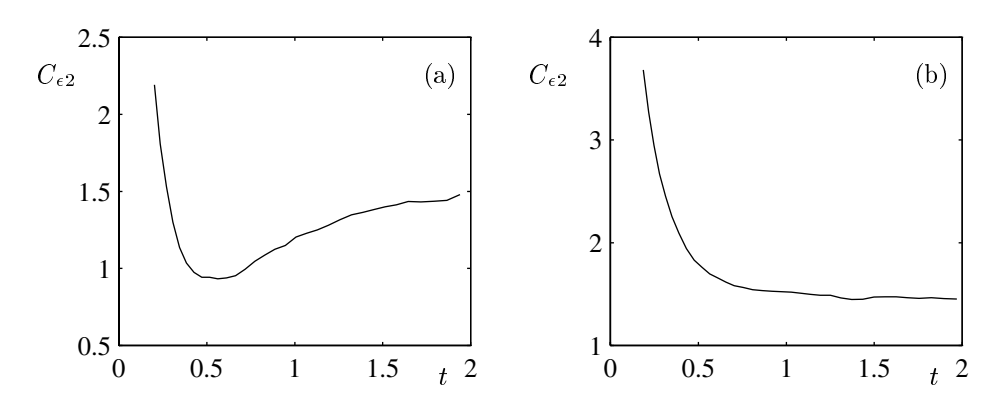


FIGURE 1 The initial behaviour of $C_{\epsilon 2}$ for a k^4 initial low wavenumber spectrum relaxed with LES using the Smagorinsky model. (a): A $k^{-5/3}$ high wavenumber spectrum. (b): A k^{-1} high wavenumber spectrum.

is constant. The larger scales have timescales which are much larger compared to the smaller scales. Hence, the small wavenumber region adjusts it self much slower to a self similar decay compared to the high wavenumbers. For high wavenumbers, at high Reynolds numbers, there should be a $k^{-5/3}$ inertial subrange in the LES. A k^2 or k^4 low wavenumber spectrum is often considered [27] as the final state of decaying turbulence, where the value of the exponent actually determines the value of $C_{\epsilon 2}$ [27]. In the simulations of Chasnov [12] a k^{-1} kinetic energy spectrum was observed in the intermediate wavenumber region. This suggests that if the initial kinetic energy spectrum is constructed with a k^{-1} slope instead of a $k^{-5/3}$ slope for the intermediate and high wavenumber region a self-similar decay will be reached faster in the simulations. In paper 4 different initial conditions are tested for both isotropic and anisotropic high Reynolds number turbulence simulations. Figures 1a,b show that the k^{-1} initial high wavenumber spectrum indeed relaxes faster to a self similar decay compared to the $k^{-5/3}$ initial spectrum.

4.2. Calibration of RANS models using LES

Standard models for the RANS approach need to be calibrated in different flows against computational or experimental data. In typical engineering flows the Reynolds number is very large. DNS yields very good predictions of various flow quantities, but can only be used at moderate Reynolds number. LES can give much higher Reynolds numbers as compared with DNS and is an important tool in RANS model calibrations.

The governing equations for the mean velocity field $U_i = \langle u_i \rangle$ is the Reynolds averaged Navier-Stokes equations. These equation contain an additional unknown term, the 'Reynolds stress tensor'

$$R_{ij} = \langle u_i' u_j' \rangle, \tag{69}$$

which carries the information about the fluctuating velocity field $u_i' = u_i - U_i$. This term has to be modelled, either directly through the mean velocity field or through additional transport equations for e.g. the turbulence kinetic energy K and the dissipation rate ϵ . However, these transport equations contain additional unknown terms which need to be modelled. A common approach is to use the transport equations for R_{ij} in the modelling

$$\left(\frac{\partial}{\partial t} + U_j \frac{\partial}{\partial x_j}\right) R_{ij} = \mathcal{P}_{ij} + \Pi_{ij} - \epsilon_{ij} - \frac{\partial}{\partial x_m} \left(J_{ijm} - \nu \frac{\partial R_{ij}}{\partial x_m}\right), \tag{70}$$

where \mathcal{P}_{ij} is the production tensor, Π_{ij} is the pressure-strain rate tensor, ϵ_{ij} is the dissipation rate tensor and J_{ijm} is the turbulence transport tensor. \mathcal{P}_{ij} produces turbulence energy through the interaction with the mean velocity field and needs no modelling, Π_{ij} redistributes energy between different components through pressure fluctuations, J_{ijm} gives spatial redistributions through turbulent transport and ϵ_{ij} dissipates turbulence kinetic energies into heat. For a more detailed description see e.g. [27]. The equation (70) can either be solved directly, with models for the new unknown terms, or be used to derive simpler models, e.g. the explicit algebraic Reynolds stress model by Wallin and Johansson [66].

In many flows, e.g. strongly strained flows and flows subjected to system rotation, the pressure-strain rate term

$$\Pi_{ij} = \frac{2}{\rho} \langle p' s'_{ij} \rangle \tag{71}$$

is very important and determines to a large extent the degree of anisotropy of R_{ij} . It is hence a key term in turbulence modelling. From the formal solution of the the pressure, through the Poisson equation, it can be divided into a rapid part, which responds directly to changes in the mean velocity field, and a slow part, which is related to the fluctuating field. The pressure-strain rate is divided accordingly. In the absence of mean velocity gradients the rapid part of Π_{ij} vanishes and the slow part equals the total pressure strain rate. Models for the slow-pressure strain rate may hence be calibrated in LES of decaying anisotropic homogeneous turbulence.

From LES only the filtered velocity field is available for direct computation of turbulence statistics. In calibrations of turbulence models it is important that the contribution from the subgrid-scales is small. In paper 1 it is shown that the contribution to the pressure-strain rate is dominated by the large scales, and is well suited for LES to compute, and for simulations with the filter scale in the inertial sub-range, which is isotropic, good high Reynolds number predictions can be obtained. The direct effect of the SGS stress model on a statistical quantity

is usually low, except for the dissipation rate, since it represents the action of the small scales. The indirect effect, through the resolved velocity field may be of greater importance, and should when possible be checked e.g. by an increase in physical resolution.

4.3. Numerical experiments of turbulence inertial range dynamics

Homogeneous flows are frequently used to study turbulence theories. The classical turbulence theory was to a large extent founded by Kolmogorov [32],[31] who derived the famous inertial range laws for the structure functions $B_{ij...k}(\mathbf{r}) = \langle \delta u_i \delta u_j \cdots \delta u_k \rangle$, where $\delta u_i = u_i(\mathbf{x} + \mathbf{r}) - u_i(\mathbf{x})$. Denote by u_l a velocity component parallel to the separation \mathbf{r} , and by u_t a velocity component orthogonal to \mathbf{r} . For high Reynolds numbers it follows from dimensional arguments that

$$B_{ll} = C \left(\epsilon r\right)^{2/3} \tag{72}$$

for inertial range separations r, where C is a constant (no summation over repeated indices 'l' and 't'). The spectral equivalent to (72) is the well known $k^{-5/3}$ law for the kinetic energy spectrum. For statistically stationary and globally isotropic turbulence Kolmogorov derived, from the Navier-Stokes equations, the Kolmogorov equations from which it follows

$$B_{lll} = -\frac{4}{5}\epsilon r,\tag{73}$$

$$B_{ltt} = -\frac{4}{15}\epsilon r. (74)$$

Lindborg [40] used the generalized Kolmogorov equations, which contains additional time derivative terms, to show that the theories also are valid in globally homogeneous and locally isotropic turbulence. Later the conditions were relaxed even further by Hill [29] and Lindborg [42] to only require locally homogeneous and locally isotropic turbulence. The classical theories require both high Reynolds numbers and that the time derivative terms should be negligible to be valid [41], [1]. In decaying turbulence at finite Reynolds numbers the time derivative term reduces the effective range in the simulation where the inertial laws are valid. Therefore it is preferable to perform turbulence simulations which are statistically stationary. This requires a production term which can balance the dissipation term in (67). The turbulence can in homogeneous flows be driven by either mean velocity gradients or a volume force to yield statistically stationary states. The latter is the most commonly used in the literature since simulations with mean velocity gradients are associated with the difficult numerical issue of re-meshing strongly strained meshes [26]. Forcing methods for homogeneous turbulence do usually not try to capture any actual turbulence generating mechanism that occur in nature. This means that the development of the large scale structures is of little interest in these cases, and besides generating large scale turbulence fluctuations the forcing should have as little effect on the flow as possible.

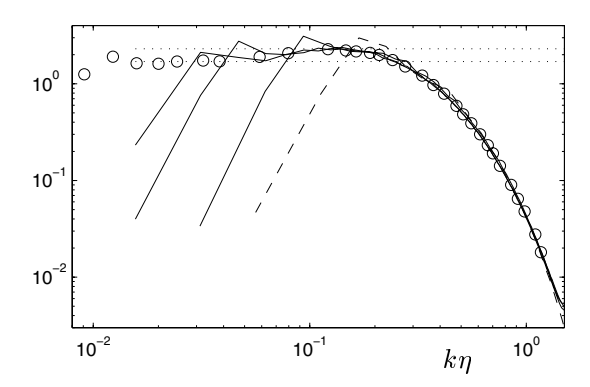


FIGURE 2 The stationary state of $E(k)\epsilon^{-2/3}k^{5/3}$ for forced homogeneous simulations at different Reynolds numbers $R=P^{1/3}k_f/\nu$, R=10.7 (dashed line), R=23.0, 59.0 and R=101.3 (solid lines), and the simulation by Yeung and Zhou[67] (circles). This is compared with the values 2.3 and 1.7 (dotted lines).

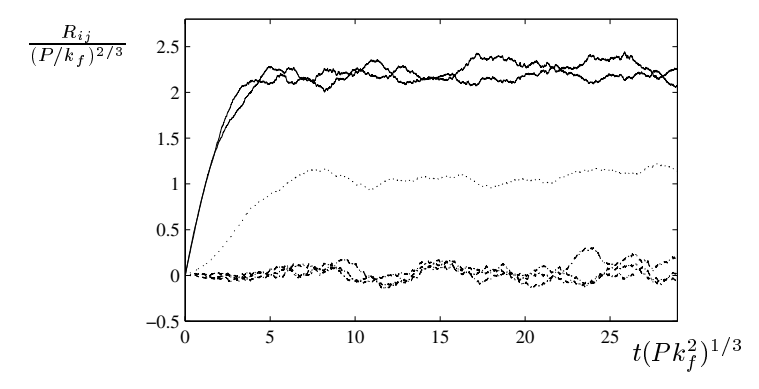
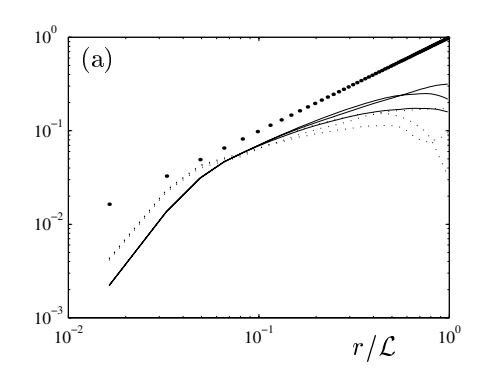


FIGURE 3 The Reynolds stress components, R_{11} , R_{22} (solid lines), R_{33} (dotted line), R_{12} , R_{23} and R_{31} (dashed dotted lines) for a forced simulation of anisotropic axisymmetric turbulence at R = 10.7.

In paper 2 a new random forcing procedure is developed and tested. By using a random volume force which is uncorrelated in time the power input P is determined solely by the force-force correlation, and can be determined a priori. The forcing is concentrated at wavenumber k_f and is neutral in the sense that it does not correlate with any turbulent structure. Figure 2 shows that the beginning of an inertial subrange may be perceived in DNS forced at the largest scales with the present methodology. Also the shape of the kinetic energy spectrum for wavenumbers greater than the forcing wavenumber seems to be relatively universal and insensitive of the forcing procedure. With the random



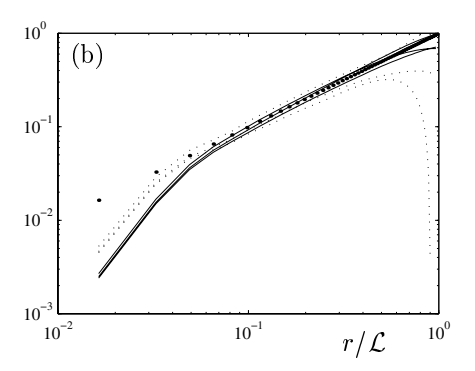


FIGURE 4 The two-point correlations $-5B_{lll}/(4\epsilon\mathcal{L})$, l=1,2,3 (solid curves), $-15B_{ltt}/(4\epsilon\mathcal{L})$ (small dotted curves) and the curve r/\mathcal{L} (large dots). \mathcal{L} is the side length of the computational box. (a): Decaying turbulence. (b): Forced turbulence.

forcing approach it is also possible to generate globally anisotropic turbulence states (figure 3).

In paper 3 the random forcing procedure is used in statistically stationary anisotropic homogeneous LES, with a large number of spectral modes (256^3) in order to resolve the non-linear dynamics of the turbulence. Corresponding decaying LES were also carried out. Figure 4 shows the third order structure functions B_{ll} and B_{lt} , from the two cases. The decaying simulation clearly fails to reproduce the well known inertial laws due to the influence of the time derivative term. The forced simulation, however, yields excellent agreement, and the advantage with the forcing method is clear. This effect is also demonstrated for isotropic turbulence in paper 2. The possibility to generate globally anisotropic states allows for the study of the inertial range behaviour for the two-point pressure velocity correlation in globally anisotropic flows. From the simulations in Paper 3 the new theories of Lindborg [40] and Hill [29] are for the first time given a numerical verification.

LES and DNS of turbulent channel flow

5.1. Turbulent plane channel flow

The turbulent plane channel flow incorporates the effect of mean shear and solid boundaries, and still allows simple implementation of accurate discretizations. Standard pseudo-spectral methods may be used in the discretization procedure. The flow is statistically stationary and may hence yield results that are independent of artificial initial conditions. The plane channel is considered to be infinitely long and wide, with the characteristic large scale determined by the distances of the walls. In a numerical simulation periodic boundary conditions are used in the streamwise and spanwise directions. In order for this numerical artifact not to affect the flow the computational domain has to be large enough so that two-point correlations are small for large separations.

The turbulence in the plane channel flow is characterized by the wall friction Reynolds number $Re_{\tau} = \delta u_{\tau}/\nu$, where δ is half the channel width and $u_{\tau} = (\nu |\mathrm{d}U/\mathrm{d}y|_{\mathrm{wall}})^{1/2}$ is the wall friction velocity. At high Reynolds numbers there is believed to exist a so called logarithmic region where the mean velocity exhibits the logarithmic profile $U/u_{\tau} = 1/\kappa \log (yu_{\tau}/\nu) + C$, where κ is the von Karman constant and C is the logarithmic intercept.

The first computation of the turbulent plane channel flow was actually an LES, performed by Deardorff [17] who used synthetic boundary conditions in the log-layer instead of the natural no-slip condition at the wall. Later, in the LES of Moin & Kim [50], the wall region was explicitly computed to yield detailed information about the turbulent structures. The first well resolved DNS (at $Re_{\tau}=180$) was presented in the landmark paper by Kim et al. [30]. The Reynolds number was increased up to $Re_{\tau}=590$ in the recent DNS by Moser et al. [51].

5.1.1. The effect of system rotation. The effect of curvature and rotation are important in many flows, e.g. in all turbo-machinery. The two effects are somewhat similar in nature. By adding system rotation in the spanwise direction in the plane channel flow, the effect of rotation can be studied with simple and accurate methods. This effect enters into the governing equations as a Coriolis term, which divides the channel into a stable side, where the turbulence is suppressed, and an unstable side, where the turbulence is enhanced (figure 1). The importance of the Coriolis term is usually measured by the rotation number

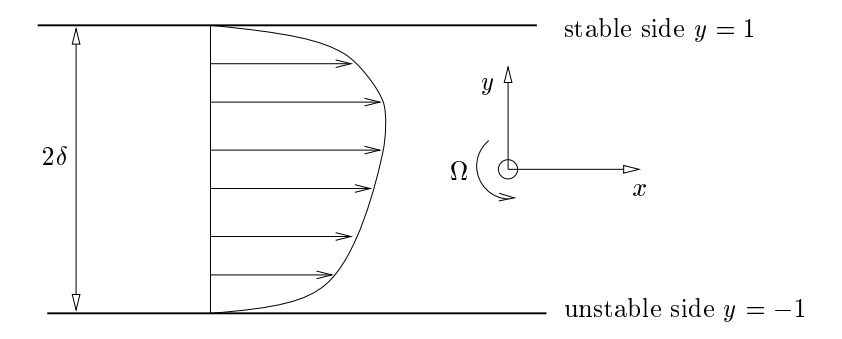


FIGURE 1 The rotating channel flow

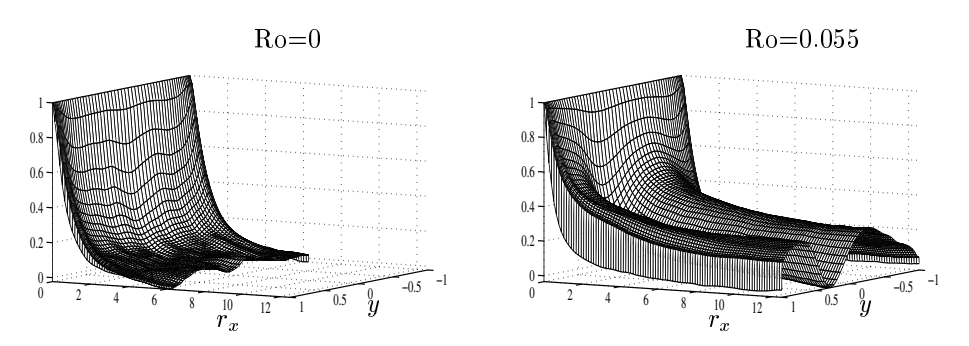


FIGURE 2 The normalized two-point correlation of fluctuating streamwise velocities for separations r_x in the x-direction as a function of y.

Ro = $2\delta\Omega/U_m$, where U_m is the mean bulk velocity and Ω is the system angular velocity. The behaviour of the turbulence statistics are rather complicated, and is a true challenge for a statistical model to capture. The rotating channel flow has been computed by several authors [33],[35]. However, the effect of the domain size has not been negligible in these computations.

For certain rotation rates the interaction of the turbulence is enforced by the Coriolis force in such a way that very long elongated structures are formed. In paper 6 Simulations at the Reynolds numbers $Re_{\tau}=130,\ 180,\ 360$ and various rotation numbers were carried out. For the highest Reynolds number $384\times257\times240$ grid points was used in the streamwise, wall-normal and spanwise directions on a $4\pi\delta\times2\delta\times4\pi\delta/3$ domain. For the critical rotation numbers associated with long structures a $8\pi\delta\times2\delta\times3\pi\delta$ domain was used. Figure 2 shows the two-point correlation in the streamwise direction of the streamwise

fluctuating velocity plotted for separations up to half the channel length for both non-rotating and rotating (Ro=0.055) flows at $Re_{\tau}=180$. Here, the long structures in the Ro=0.055 case show up as persistent high values of the two-point correlation. In a simulation these structures have to be captured by the computational domain which strongly increases the computational effort. Even though the computational domain is twice as long $(8\pi\delta)$ in the rotating case as compared to the non-rotating case $(4\pi\delta)$ the two-point correlation still has significant values for the largest separations.

The high Reynolds number simulations are well suited for the development of SGS stress models in LES. LES quantities can be evaluated directly in *a priori* tests, and compared with actual LES results. The data base generated from the DNS will be used both for the development of SGS models for LES and for RANS-based turbulence models.

5.2. Stochastic SGS modelling

In paper 5 the stochastic model approach is used to improve the statistical properties of the SGS model. The stochastic models are added to the standard Smagorinsky model, which both numerically are treated together with non-linear terms. Since a large part of the total dissipation is treated explicitly the Chebyshev-tau method was needed to enhance the numerical stability as compared to the integration method [45]. Both a stochastic Smagorinsky parameter approach and a Schumann like model approach were used and implemented with a finite timescale of the stochastic processes. This implies that the SDE for the stochastic processes have to be solved in a Lagrangian sense and extra transport equations have been added to the code.

The stochastic terms reduce the length scale and increase the variance of the SGS dissipation and also give backscatter. The mean velocity profile is relatively insensitive to the stochastic term, while the second order moments are strongly affected. The stochastic Smagorinsky parameter approach may yield locally negative viscosity which is numerically unstable and is controlled by artificially restricting the allowed values of the negative dissipation. The Schumann approach, however, yields stable solution without restrictions.

CHAPTER 6

Concluding remarks

LES is supposed to perform well at high Reynolds numbers and for complex geometries. Complex geometries involves the implementation of more general (lower-order) methods with significantly strained and anisotropic meshes. The development of good numerical methods which in an accurate manner allows for different resolutions in different regions is needed. Also, high Reynolds numbers yield very small structures close to solid walls. Typically these cannot be resolved by LES, and the development of new boundary conditions or near wall solution procedures are essential to make LES the leading engineering tool for turbulent flows. These issues are, however, not considered in this thesis. Instead focus is put on 'well resolved' LES predictions where the numerical errors are negligible and the smallest large scale is well with in the filter scale.

From the present simulations it is seen that accurate high Reynolds number calibrations of RANS models may be achieved by LES. It is also shown that that LES can successfully be used to verify high Reynolds number turbulence theories unattainable for DNS. The developed random forcing method can be used as a tool to yield relatively high Reynolds number DNS from which SGS models can be evaluated. However, the homogeneous turbulence case is not sufficient to completely test the performance of turbulence models. The turbulent plane channel flow includes more physical effects, through the presence of the walls, and can be used to get a good qualitative knowledge about the performance of various models. A thorough parametric study of the effect of system rotation for various Reynolds numbers through DNS resulted in a large data base which can be used in the turbulence modelling process. The statistical quantities show complicated behaviour, due to the combined effects of the wall and system rotation, from which good calibrations of RANS models may be obtained. Also turbulence structures, which a good LES should be able to capture, show a relatively complicated development for the different rotation rates.

Acknowledgments

I wish to thank my supervisor Professor Arne Johansson, with whom I have had many tough tennis matches throughout the years, for guiding me into the area of turbulence. Arne has always studied my manuscripts carefully and listened to my ideas. His great knowledge in turbulence has been very useful in achieving good scientific research.

Doctor Magnus Hallbäck who took a lot of his time to discuss turbulence and numerical simulation codes with me during my first years is gratefully acknowledged. I do also want to thank Martin Skote for a great collaboration in the area of super computers in which both of us have spent a lot of time.

My colleagues at the department have provided a professional and stimulating atmosphere. I thank you all for that and for the many interesting discussions.

I would also like to thank all my friends at the department, particularly the people I have had the joy to share room with during the years. This strongly contributed to a pleasant time at the department.

Especially I wish to thank my mother and the rest of my family for their support and encouragement, and Annika for your love at all times.

Bibliography

- K. Alvelius. Random forcing of three-dimensional homogeneous turbulence. Physics of Fluids A, 11(7):1880-1889, 1999.
- [2] K. Alvelius, M. Hallbäck, and A. V. Johansson. Calibration of models for the slow pressurestrain rate using les. In *Turbulent shear flows 11*, volume 2, pages P2-107-112, 1997.
- [3] K. Alvelius, M. Hallbäck, and A. V. Johansson. Investigation of the self-consistency of the Smagorinsky constant and the value of the Rotta parameter at high Reynolds numbers. In J. P. Chollet, P. R. Voke, and L. Kleiser, editors, *Direct and Large Eddy Simulation II*, volume 5, pages 69-80, Dordrecht, The Netherlands, 1997. Kluwer.
- [4] K. Alvelius, M. Hallbäck, and A. V. Johansson. Les of decaying turbulence using a spectral method implemented on parallel computers. In C. Liu and Z. Liu, editors, Advances in DNS/LES, pages 499-506, Columbus, 1997. Greyden Press.
- [5] K. Alvelius, M. Hallbäck, and A. V. Johansson. An LES study of the self consistency of the Smagorinsky model and calibration of slow-pressure strain rate models. *European Journal of Mechanics B/Fluids*, 1999. Submitted for publication.
- [6] K. Alvelius and A. V. Johansson. LES computations and comparison with Kolmogorov theory for two-point pressure-velocity correlations and structure functions for globally anisotropic turbulence. *Journal of Fluid Mechanics*, 1999. Accepted for publication.
- [7] K. Alvelius and A. V. Johansson. Modeling of the length scale and variance of subgrid quantities in a turbulent channel flow. In Second AFOSR International Conference on Direct Numerical Simulation and Large Eddy Simulation, 1999.
- [8] J. Bardina, J. H. Ferziger, and W. C. Reynolds. Improved subgrid scale models for large eddy simulation. In AIAA 13th Fluid & Plasma Conference, July 14-16 1980.
- [9] W. Cabot. Near-wall models in large eddy simulations of flow behind a backward-facing step. Center for Turbulence Research, Annual Research Briefs, pages 199–210, 1996.
- [10] D. Carati, S. Ghosal, and P. Moin. On the representation of backscatter in dynamic localization models. *Physics of Fluids*, 7(3):606-616, 1995.
- [11] J. R. Chasnov. Simulation of the Kolmogorov inertial subrange using an improved subgrid model. Physics of Fluids A, 3(1):188–200, 1991.
- [12] J. R. Chasnov. Similarity states of passive scalar transport in isotropic turbulence. *Physics of Fluids*, 6(2):1036-1051, 1994.
- [13] J. P. Chollet. Two-point closure used for a sub-grid scale model in large eddy simulations. In F. Durst and B. Launder, editors, *Turbulent Shears Flow IV*, pages 62-72. Springer-Verlag, Heidelberg, 1984.
- [14] R. Clark, J. H. Ferziger, and W. C. Reynolds. Evaluation of subgrid-scale models using an accurately simulated flow. *Journal of Fluid Mechanics*, 91:1-16, 1979.
- [15] P. Compte, O. Métais, E. David, F. Ducros, and M. A. Gonze. Subgrid-scale models based upon the second-order structure-function of velocity. In P. R. Voke et al., editor, *Direct* and Large-Eddy Simulation I, pages 61-72. Kluwer Academic Publishers, 1994.
- [16] G. Comte-Bellot and S. Corrsin. The use of a contraction to improve the isotropy of grid-generated turbulence. *Journal of Fluid Mechanics*, 25:657-682, 1966.

- [17] J. W. Deardorff. A numerical study of three-dimensional turbulent channel flow at large Reynolds numbers. *Journal of Fluid Mechanics*, 41:453-480, 1970.
- [18] J. A. Domaradzki and E. M. Saiki. A subgrid-scale model based on the estimation of unresolved scales of turbulence. *Physics of Fluids*, 9(7):2148–2164, 1997.
- [19] P. A. Durbin and C. G. Speziale. Realizability of second-moment closure via stochastic analysis. *Journal of Fluid Mechanics*, 280:395-407, 1994.
- [20] C. A. J. Fletcher. Computational Techniques for Fluid Dynamics, Volume I. Springer-Verlag, Berlin Heidelberg, 1991.
- [21] M. Germano. Turbulence: the filtering approach. Journal of Fluid Mechanics, 238:325–336, 1992.
- [22] M. Germano, U. Piomelli, P. Moin, and W. H. Cabot. A dynamic subgrid-scale eddy viscosity model. *Physics of Fluids*, 3(7):1760-1765, 1991.
- [23] B. J. Geurts. Inverse modeling for large-eddy simulation. Physics of Fluids, 9(12):3585-3587, 1997.
- [24] S. Ghosal, T. S. Lund, P. Moin, and K. Akselvoll. A dynamic localization model for large-eddy simulation of turbulent flows. *Journal of Fluid Mechanics*, 285:229-255, 1995.
- [25] S. Ghosal and P. Moin. The basic equations for the large eddy simulation of turbulent flows in complex geometry. *Journal of Computational Physics*, 118:24–37, 1995.
- [26] M. Hallbäck. Development of Reynolds Stress Closures of Homogeneous Turbulence through Physical and Numerical Experiments. PhD thesis, KTH, 1993.
- [27] M. Hallbäck, D. S. Henningson, A. V. Johansson, and P. H. Alfredsson, editors. *Turbulence and Transition Modelling*. ERCOFTAC Series. Kluwer Academic Publishers, Dordrecht, The Netherlands, 1996.
- [28] C. Härtel and L. Kleiser. Galilean invariance and filtering dependence of near-wall grid-scale/subgrid-scale interactions in large-eddy simulation. *Physics of Fluids*, 9(2):473-475, 1997.
- [29] R. J. Hill. Applicability of Kolmogorov's and Monins's equations of turbulence. Journal of Fluid Mechanics, 353:67-81, 1997.
- [30] J. Kim, P. Moin, and R. Moser. Turbulence statistics in fully developed channel flow at low Reynolds number. *Journal of Fluid Mechanics*, 177:133-166, 1987.
- [31] A. N. Kolmogorov. Dissipation of energy in the locally isotropic turbulence. Proceedings of the Royal Society of London, Series A, 434(1991):15-17, 1941.
- [32] A. N. Kolmogorov. The local structure of turbulence in incompressible viscous fluid for very large Reynolds numbers. Proceedings of the Royal Society of London, Series A, 434(1991):9-13, 1941.
- [33] R. Kristoffersen and H. Andersson. Direct simulation of low-Reynolds-number turbulent flow in a rotating channel. *Journal of Fluid Mechanics*, 256:163–197, 1993.
- [34] Bernt Øksendal. Stochastic Differential Equations, An Introduction with Applications. Springer-Verlag, Berlin Heidelberg, fifth edition, 1998.
- [35] E. Lamballais, M. Lesieur, and O. Métais. Effects of spanwise rotation on the vorticity stretching in transitional and turbulent channel flow. *International Journal of Heat and Fluid Flow*, 17:324-332, 1996.
- [36] C. E. Leith. Stochastic backscatter in a subgrid-scale model: Plane shear mixing layer. Physics of Fluids A, 2(3):297-299, 1990.
- [37] M. Lesieur and O. Métais. New trends in large-eddy simulations of turbulence. Annual review of Fluid Mechanics, 28:45-83, 1996.
- [38] D. K. Lilly. The representation of small-scale turbulence in numerical simulation experiments. In Proceedings of the IBM Scientific Computing Symposium on Environmental Science, IBM Form No. 320-1951, page 195, 1967.
- [39] D. K. Lilly. A proposed modification of the Germano subgrid-scale closure method. Physics of Fluids A, 4(3):633-635, 1992.

- [40] E. Lindborg. A note on Kolmogorov's third order structure function law, the local isotropy hypothesis and the pressure-velocity correlation. *Journal of Fluid Mechanics*, 326:343–356, 1996.
- [41] E. Lindborg. Correction to the four-fifths law due to variations of the dissipation. Physics of Fluids, 11(3):510-512, 1999.
- [42] E. Lindborg. The pressure terms in the general Kolmogorov equation. *Physics of Fluids*, 1999. Submitted for publication.
- [43] S. Liu, C. Meneveau, and J. Katz. Experimental study of similarity subgrid-scale models of turbulence in the far-field of a jet. In P. R. Voke et al., editor, *Direct and Large-Eddy Simulation I*, pages 37-48. Kluwer Academic Publishers, 1994.
- [44] T. S. Lund and H.-J. Kaltenbach. Experiments with explicit filtering for LES using a finite-difference method. Center for Turbulence Research, Annual Research Briefs, pages 91-105, 1995.
- [45] A. Lundbladh, D. S. Henningson, and A. V. Johansson. An efficient spectral integration method for the solution of the Navier-Stokes equations. Technical Report FFA TN 1992-28, Flygtekniska Försöksanstalten, 1992.
- [46] P.J. Mason and D. J. Thomson. Stochastic backscatter in large-eddy simulations of boundary layers. *Journal of Fluid Mechanics*, 242:51-78, 1992.
- [47] C. Meneveau. Statistics of turbulence subgrid-scale stresses: Necessary conditions and experimental tests. Physics of Fluids, 6(2):815–833, 1994.
- [48] C. Meneveau, T. S. Lund, and W. H. Cabot. A Lagrangian dynamic subgrid-scale model of turbulence. *Journal of Fluid Mechanics*, 319:353-385, 1996.
- [49] O. Métais and M. Lesieur. Spectral large-eddy simulation of isotropic and stably stratified turbulence. *Journal of Fluid Mechanics*, 239:157-195, 1992.
- [50] P. Moin and J. Kim. Numerical investigation of turbulent channel flow. *Journal of Fluid Mechanics*, 118:341, 1982.
- [51] R. Moser, J. Kim, and N. N. Mansour. Direct numerical simulation of turbulent channel flow up to $Re_{\tau} = 590$. Physics of Fluids, 11(4):943–945, 1999.
- [52] M. Olsson. Large Eddy Simulation of Turbulent Jets. PhD thesis, KTH, January 1997.
- [53] M. Olsson and L. Fuchs. Large eddy simulation of the proximal region of a spatially developing circular jet. *Physics of Fluids*, 8(8):2125-2137, 1996.
- [54] U. Piomelli and J. Liu. Large-eddy simulations of rotating channel flows using a localized dynamic model. *Physics of Fluids*, 7(4):839-848, 1995.
- [55] U. Piomelli, Y. Yunfang, and A. J. Ronald. Subgrid-scale energy transfer and near-wall turbulence structure. *Physics of Fluids*, 8(1):215-224, 1996.
- [56] O. Reynolds. An experimental investigation of the circumstances which determine whether the motion of water shall be direct or sinuous, and the law of resistance in parallel channels. Philosophical Transactions of the Royal Society of London, 174:935-982, 1883.
- [57] F. Sarghini, U. Piomelli, and E. Balaras. Scale-similar models for large-eddy simulations. Physics of Fluids, 11(6):1596-1607, 1999.
- [58] U. Schumann. Stochastic backscatter of turbulence energies and scalar variance by random subgrid-scale fluxes. Proceedings of the Royal Society of London, Series A, 451:293-318, 1995.
- [59] A. Scotti, C. Meneveau, and D. K. Lilly. Generalized Smagorinsky model for anisotropic grids. Physics of Fluids A, 5(9):2306-2308, 1993.
- [60] T. Sjögren and A. V. Johansson. Measurements and modelling of homogeneous axisymmetric turbulence. *Journal of Fluid Mechanics*, 374:59-90, 1998.
- [61] J. Smagorinsky. General circulation experiments with the primitive equations. Monthly Weather Review, page 99, 1963.

- [62] A. Sohankar, L. Davidson, and C. Norberg. A dynamic one-equation subgrid model for simulation of flow around a square cylinder. In W. Rodi and D. Laurence, editors, Engineering Turbulence Modelling and Experiments 4, pages 227-236. Elsevier, 1999.
- [63] C. G. Speziale. Galilean invariance of subgrid-scale stress models in the large eddy simulation of turbulence. *Journal of Fluid Mechanics*, 156:55-62, 1985.
- [64] H. Tennekes and J. L. Lumley. A First Course in Turbulence. The MIT Press, Cambridge, Massachusetts, and London, England, 1992.
- [65] B. Vreman, B. Geurts, and H. Kuerten. Realizability conditions for the turbulent stress tensor in large-eddy simulation. *Journal of Fluid Mechanics*, 278:351–362, 1994.
- [66] S. Wallin and A. V. Johansson. A complete explicit algebraic Reynolds stress model for incompressible and compressible turbulent flows. 1999. Submitted for publication.
- [67] P. K. Yeung and Y. Zhou. Universality of the Kolmogorov constant in numerical simulations of turbulence. *Physical Review E*, 56(2):1746-1752, 1997.
- [68] A. Yoshizawa. Eddy-viscosity-type subgrid-scale model with a variable Smagorinsky coefficient and its relationship with the one-equation model in large eddy simulation. *Physics of Fluids A*, 3(8):2007–2009, 1991.